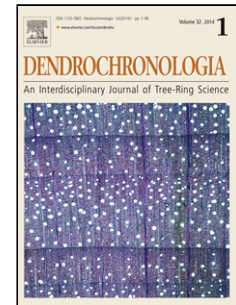


## Accepted Manuscript

Title: A novel stochastic method for reconstructing daily precipitation times-series using tree-ring data from the western Canadian Boreal Forest

Authors: K.P. Chun, S.D. Mamet, J. Metsaranta, A. Barr, J. Johnstone, H. Wheeler



PII: S1125-7865(16)30085-6  
DOI: <http://dx.doi.org/doi:10.1016/j.dendro.2017.01.003>  
Reference: DENDRO 25418

To appear in:

Received date: 9-8-2016  
Revised date: 7-1-2017  
Accepted date: 23-1-2017

Please cite this article as: Chun, K.P., Mamet, S.D., Metsaranta, J., Barr, A., Johnstone, J., Wheeler, H., A novel stochastic method for reconstructing daily precipitation times-series using tree-ring data from the western Canadian Boreal Forest. *Dendrochronologia* <http://dx.doi.org/10.1016/j.dendro.2017.01.003>

This is a PDF file of an unedited manuscript that has been accepted for publication. As a service to our customers we are providing this early version of the manuscript. The manuscript will undergo copyediting, typesetting, and review of the resulting proof before it is published in its final form. Please note that during the production process errors may be discovered which could affect the content, and all legal disclaimers that apply to the journal pertain.

**A novel stochastic method for reconstructing daily precipitation times-series using tree-ring data from the western Canadian Boreal Forest**

K. P. Chun<sup>a,b</sup>, S.D. Mamet<sup>b,c</sup>, J. Metsaranta<sup>d</sup>, A. Barr<sup>e</sup>, J. Johnstone<sup>b</sup>, and H. Wheeler<sup>b</sup>

<sup>a</sup> Department of Geography, Honk Kong Baptist University, Kowloon Tong, Hong Kong (KP Chun: kpchun@hkbu.edu.hk)

<sup>b</sup> Global Institute for Water Security, University of Saskatchewan, National Hydrology Research Centre, 11 Innovation Boulevard, Saskatoon, SK S7N 3H5, Canada (SD Mamet: steven.mamet@usask.ca, J Johnstone: jill.johnstone@usask.ca, H Wheeler: howard.wheater@usask.ca)

<sup>c</sup> Department of Soil Science, University of Saskatchewan, 51 Campus Drive, University of Saskatchewan, Saskatoon, SK S7N 5A8, Canada

<sup>d</sup> Canadian Forest Service, Natural Resources Canada, Northern Forestry Centre, 5320-122 Street, Edmonton, AB T6H 3S5, Canada (J Metsaranta: juha.metsaranta@canada.ca)

<sup>e</sup> Environment Canada, University of Saskatchewan, National Hydrology Research Centre, 11 Innovation Boulevard, Saskatoon, SK S7N 3H5, Canada (A Barr: alan.barr@canada.ca)

<sup>a</sup> **Corresponding author:** KP Chun (+852 3411 6541)

**Abstract**

Tree ring data provide proxy records of historical hydroclimatic conditions that are widely used for reconstructing precipitation time series. Most previous applications are limited to annual time scales, though information about daily precipitation would enable a range of additional analyses of environmental processes to be investigated and modelled. We used statistical downscaling to simulate stochastic daily precipitation ensembles using dendrochronological data from the western Canadian boreal forest. The simulated precipitation series were generally consistent with observed precipitation data, though reconstructions were poorly constrained during short periods of forest pest outbreaks. The proposed multiple temporal scale precipitation reconstruction can generate annual daily maxima and persistent monthly wet and dry episodes, so that the observed and simulated ensembles have similar precipitation characteristics (i.e. magnitude, peak, and duration)—an improvement on previous modelling studies. We discuss how ecological disturbances may limit reconstructions by inducing non-linear responses in tree growth, and conclude with suggestions of possible applications and further development of downscaling methods for dendrochronological data.

**Keywords:** tree rings; statistical downscaling; boreal forest; stochastic precipitation generation; droughts

## Introduction

Precipitation is a fundamental driver for both ecological and anthropogenic systems. Yet our understanding of historical precipitation patterns is typically limited to annual time scales and many records of daily precipitation are spatial heterogeneous and temporally discontinuous (Razavi et al., 2015). Tree rings provide information about low frequency (i.e., decadal) climate oscillations and drought severity, and have facilitated reconstruction of historical precipitation across North America (Cook et al., 2015). Precipitation reconstructions are commonly developed using correlation analysis in the time domain (Touchan et al., 1999) and spectral analysis in the frequency domain (Meko et al., 1985). Advanced time series approaches, such as wavelet techniques, have also become common for analysing tree ring and precipitation data in both the time and frequency domains simultaneously (Gray et al., 2003). However, shorter time periods, e.g., 30 years, can be truly misleading in calculating the statistical properties of precipitation time series, due to extensive non-stationarities observed in this time frame, highlighting the difficulty in reconstructions that employ short instrumental climate records (Razavi et al., 2015). Moreover, and in spite of the success in using dendrochronological records for annual reconstructions (e.g. Biondi, 2014), daily precipitation reconstructions are non-existent to our knowledge. Therefore, in order to generate accurate, high-resolution precipitation time series, reconstruction techniques must be able to simulate both the underlying stochastic process in the time series and incorporate non-stationarities in the first-order (e.g., mean) and second-order (e.g., variance and autocorrelation) statistical properties (Elshorbagy et al., 2016; Razavi et al., 2015, 2016).

Statistical downscaling is used to generate fine-scale time series from coarse numerical model outputs (Maraun et al., 2010). Downscaling uses historical data to establish relationships among different time scales and employs these empirical associations to

generate fine scale time series using coarse-scale data as proxies (Chun, 2010). For example, we can generate daily precipitation time series using coarse climate model outputs and/or low frequency climate oscillations (Chandler and Wheeler, 2002; Chun et al., 2013). These daily time series may help to understand environmental hazards such as flooding (Chun, 2010; Yang et al., 2006), and provide important information for placing climate variability in a historical context (Bradley, 2015). Here we propose a novel method that incorporates ring-width time series to reconstruct daily precipitation using downscaling (Chandler and Wheeler, 2002). We analysed the simulated daily precipitation properties, including persistence characteristics (Biondi et al., 2002) and annual daily extremes (Chun, 2010) at multiple temporal scales, in order to simulate daily precipitation sequences using tree rings.

Dendroclimatological studies typically analyse growth at frequencies of several months to years, thereby integrating over consecutive episodes of cambial cell division and radial growth. This is a time horizon that may cover distinct changes in soil moisture as caused by fluctuating precipitation intensities (Au and Tardif, 2012; Chen et al., 2017; Köcher et al., 2012). Periods of rainfall followed by infiltration into the soil may take hours to reach the absorbing roots and physiologically significant increases in soil moisture may only occur after larger events and with a delay, if soil hydraulic conductivity is low. Tree rings do not incorporate a resolvable daily precipitation signal (Köcher et al., 2012). However, tree ring data do incorporate coarse scale (i.e., monthly and seasonal) precipitation information (Girardin and Tardif, 2005; Hofgaard et al., 1999; Huang et al., 2010) that may be used in simulations of underlying stochastic processes and non-stationarities in statistical properties into finer scale reconstructions of hydrological variables (Razavi et al., 2015, 2016). As a case study for our empirical downscaling approach, we used tree rings from the three most widespread boreal tree species across western Canada: trembling aspen (*Populus tremuloides* Michx.), jack pine (*Pinus banksiana* Lamb.), and black spruce (*Picea mariana*

[Mill.] B.S.P. Our goal was not paleoclimate reconstruction *sensu stricto*, but to provide a methodology for obtaining the necessary parameters to reconstruct daily precipitation ensembles. Here we used coarse-scale tree-ring data from these species to generate fine-scale daily precipitation ensembles, and provide the details of the data, downscaling methods, and their evaluation approaches.

## Material and Methods

### *Site description*

The study was undertaken at the Boreal Ecosystem Research and Monitoring Sites (BERMS; Griffis et al., 2003) located near the southern edge of the Boreal Plains Ecozone (Figure 1). Three sites were sampled: Old Aspen (OA), Old Black Spruce (OBS), and Old Jack Pine (OJP). More details of the three BERM sites can be found in Barr et al. (2012). The mean annual temperature of the area is around 3 to 4 °C with high seasonal and inter-annual variation (Ireson et al., 2015). Moisture stress is expected to increase (i.e., declining P-PET, precipitation minus potential evapotranspiration) under a warming climate (Ireson et al., 2015). Three main regional tree species (aspen, jack pine, and black spruce) represent the dominant land cover types of western Canadian boreal forests (Hall et al., 1997).

### Target tree species

The dendroclimatic response of aspen has been intensively studied in Canada (e.g., Chhin and Wang, 2016; Hogg et al., 2005; Huang et al., 2010; Huang et al., 2013; Lapointe-Garant et al., 2010; Leonelli et al., 2008), and drought, insects and pathogens may contribute to widespread decline in aspen growth. Defoliation and drought events also leave aspen more susceptible to secondary attack by the wood-boring large aspen tortix (*Choristoneura conflictana* [Wlk.]), the poplar peniophora fungus (*Peniophora polygonia* [Pers.:Fr.] Boud., and *Armillaria* root disease (Hogg et al., 2005). Widespread mortality is predicted for aspen

across its southern range due to a combination of climate change, and biotic and abiotic influences (Rehfeldt et al., 2009).

Jack pine is the most widely distributed pine species in Canada (Burns and Honkala, 1990), but in spite of its apparent climatic sensitivity, it has not received widespread attention in boreal forest precipitation reconstructions (one exception is Pisaric et al., 2009). While jack pine is a drought-tolerant species due to deep tap roots, it has shown sensitivity to drought (Mamet et al., 2015), a signal that is evident in spite of periodic defoliation by jack pine budworm (*Choristoneura pinus pinus* Free.) (Volney, 1998) and *Armillaria infection* (Mallett and Volney, 1990). Thus jack pine offers considerable promise for precipitation reconstruction, which is particularly useful in light of the drought-induced growth decline predicted for most of Canada (Peng et al., 2011).

Black spruce is a wide-ranging, abundant conifer in the northern parts of North America (Viereck and Johnston, 1990). Though black spruce typically grows in wet environments, evidence suggests that drought impacts on black spruce may be more widespread than previously thought (e.g. Girardin et al., 2016; Walker and Johnstone, 2014). Drought stress in black spruce is likely related to drying of organic topsoil where most of the roots are located (Pepin et al., 2002). In addition to climate, spruce budworm (*Choristoneura fumiferana* Clemens) has increasingly affected spruce growth in the 20<sup>th</sup> century (Sonia et al., 2011), more so in drier upland stands (Lacey and Dech, 2012) and in conjunction with *Armillaria* infection (Westwood et al., 2012). However, black spruce is at much lower risk for defoliation due to its northern range, relative to more southern species (Drobyshev et al., 2010) and budworm preference for balsam fir (*Abies balsamea* [L.] (Gray, 2013).

### *Tree ring field data design and collection*

In 2011 and 2012, we sampled tree rings from aspen, jack pine, and black spruce from mature stands surrounding flux towers at the three BERMS sites (Figure 1). We sampled one or two breast height increment cores from all living trees within six 10x10 m plots at each site. All samples (66 aspen from OA, 187 black spruce from OBS, and 197 jack pine from OJP; N = 450) were dried and sanded with progressively finer sandpaper until individual xylem cells were visible. We measured ring-widths with WinDendro (Regent Instruments, Québec, Canada) and cross-dated ring-width chronologies from each tree within a site visually and statistically using COFECHA (Holmes, 1992).

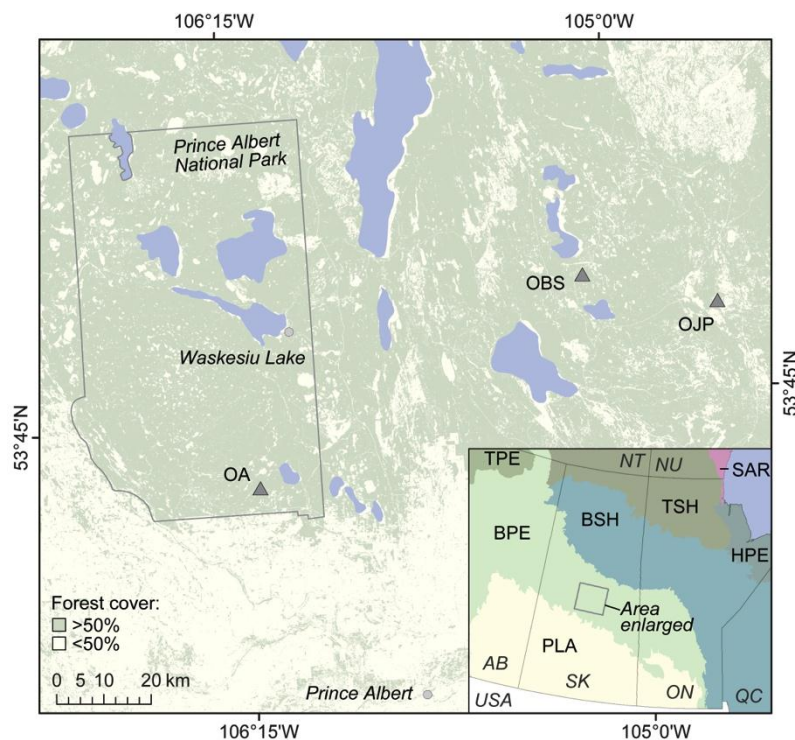


**Figure 1.** The location of the Old Aspen (OA), Old Black Spruce (OBS), and Old Jack Pine (OJP) flux towers (triangles) in the Boreal Plains Ecozone (BPE) of central Saskatchewan. Adjusted and Homogenized Canadian Climate Data (AHCCD; Vincent et al., 2012) were obtained from Waskesiu Lake in Prince Albert National Park (outlined) and Prince Albert. The green area represents >50% forest cover compared to beige (<50% forest cover) as determined by Hansen et al. (2013). Inset map shows location of the study area in relation to ecozones: TPE = Taiga Plains, PLA = Plains, BSH = Boreal Shield, TSH = Taiga Shield, HPE = Hudson Plains, SAR = Southern Arctic, and provincial boundaries: Alberta (AB), Saskatchewan (SK), Ontario (ON), Québec (QC), Northwest Territories (NT) and Nunavut (NU).

### *Regional curves*

We derived a single “master” tree-ring chronology (Biondi, 2014; Fritts, 2001) from tree ring measurements at our study sites, encompassing the three dominant species in the region. The

growth trend of each tree ring width chronology was first removed using a cubic smoothing spline with 50% frequency response of the time series, as implemented in the dendrochronology program library in R (dplR; Bunn et al., 2014). Two master tree-ring chronologies were tested as potential proxies for reconstructing regional precipitation ensembles:

- a. MC1: All trees together without considering their tree species
- b. MC2: A master curve derived for each tree species (Figures 2a–2c) followed by averaging of each species-specific series into a master tree ring chronology (Figure 2d)

Both candidate master series (MC1 and MC2) showed a highly correlated pattern of inter-annual variation ( $R^2=0.9$ ). Therefore, we used only the master curve resulting from the average of the three tree species (MC2) in further analyses (Table 1).

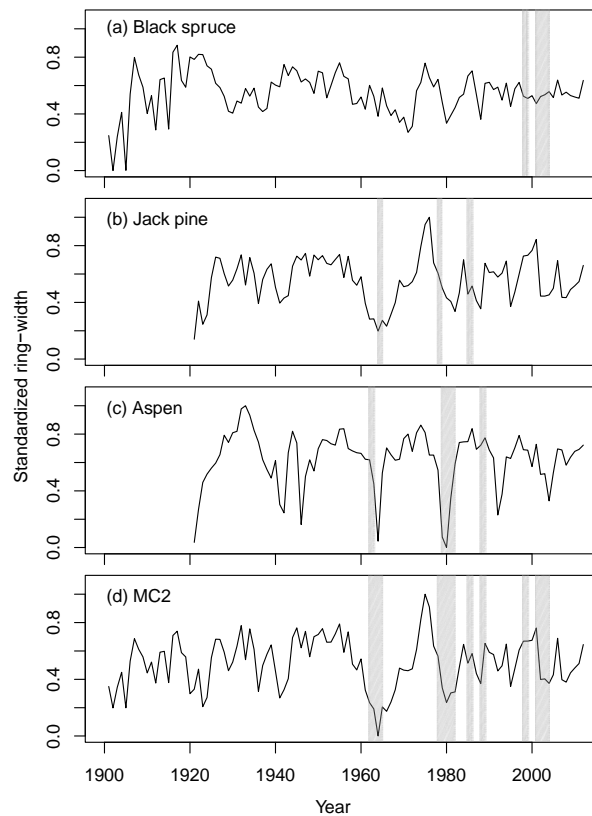


**Figure 2.** Standardized ring width chronologies for (a) black spruce, (b) jack pine, (c) aspen, and (d) MC2: a master chronology derived by averaging the three species curves. Shaded regions indicate historical periods of high pest activity within Saskatchewan: (a) Spruce budworm, (b) Jack pine budworm, (c) Forest tent caterpillar, and (d) all pests combined (Hogg et al., 2005; National Forestry Database, 2015; from Volney, 1988).

To provide some temporal context to conspicuous departures in tree growth, we obtained historical records of pest activity within Saskatchewan and compared these to the master chronologies (Figure 2). These included the spruce budworm, the jack pine budworm, and the forest tent caterpillar (Hogg et al., 2005; National Forestry Database, 2015; Volney, 1988). Due to the discontinuous nature of the various outbreak records (e.g., missing recent decades), we did not use these data to condition our downscaling models, only to identify some potential non-climatic growth departures in our master chronologies.

**Table 1** Statistical characteristics of standardized chronologies produced from trees established near the Old Black Spruce, Old Jack Pine, and Old Aspen flux towers in the Boreal Plains Ecozone of central Saskatchewan.

Species	No. trees	Start	End	No. years	MSI <sup>a</sup>	AR1 <sup>b</sup>	EPS <sup>c</sup>
Black spruce	187	1889	2012	123	0.411	0.434	0.973
Jack pine	197	1916	2012	96	0.481	0.583	0.986
Aspen	66	1915	2012	97	0.438	0.499	0.971
MC2	450	1889	2012	123	0.495	0.509	0.986

<sup>a</sup> Mean series inter-correlation.

<sup>b</sup> Mean first order correlation present in the standardized ring-width series.

<sup>c</sup> Expressed population signal, which represents the degree to which a particular sampling portrays the hypothetical perfect chronology (Briffa and Jones, 1990).

### *Climate data and indices*

Precipitation data between 1996 and 2010 from the three BERM sites were used for development and calibration of the downscaling methods. Precipitation was recorded using Belfort 3000 precipitation gauges (Belfort Instrument, Baltimore, ML, <http://belfortinstrument.com>) at each of the three sites (Barr et al., 2012). The gauges were located in small forest clearings and shielded by Alter shields. The wind speed at gauge height never exceeded  $1.5 \text{ m s}^{-1}$ , so that wind-induced undercatch was minimal.

To understand the effects of low frequency (i.e., decadal) climate signals on precipitation reconstructions, we used ten teleconnection indices obtained from the rotated principal component analysis of monthly mean standardized 500 hPa height anomalies (Barnston and Livezey, 1987). The ten indices can be roughly divided into two groups related to Pacific and Atlantic climate oscillations (Table 2).

**Table 2.** Data schedule of the ten teleconnection indices are extracted from the Climate Prediction Center (CPC) of the US National Weather Service (NWS). Teleconnection patterns were derived from the 1950-2000 base period, and a varimax rotation was applied to the top ten leading un-rotated modes for different calendar months. Therefore, the explained variance for each mode was different for each month. Further details of teleconnection pattern computation procedures can be found at <http://www.cpc.ncep.noaa.gov/data/teledoc/telepatcalc.shtml>.

North Pacific Indices	
West Pacific Pattern	WP
East Pacific/North Pacific Pattern	EP/NP
Pacific/North American Pattern	PNA
Tropical/Northern Hemisphere Pattern	TNH
Pacific Transition Pattern	PT
North Atlantic Indices	
North Atlantic Oscillation	NAO
East Atlantic Pattern	EA
East Atlantic/West Russia Pattern	EA/WR
Scandinavia Pattern	SCA
Polar/Eurasia Pattern	POL

For long-term evaluation of the downscaling methods, we used two time series from the Adjusted and Homogenized Canadian Climate Data (AHCCD) products (Vincent et al., 2012), from Prince Albert (station 4056240) between 1889 and 2012 and Waskesiu Lake (station 4068559) between 1966 and 2012 (Figure 1). AHCCD products are derived from Canadian weather stations, and contain controlled, adjusted, or homogenised records that are suitable for climate studies (Vincent et al., 2012). In addition, we used a third long-term time series extracted from the Canadian Gridded Temperature and Precipitation anomalies (CANGRD) product between 1900 and 2012, which is a gridded AHCCD set in a 50km polar stereographic projection (Milewska et al., 2005).

### *Reconstruction approaches*

Our reconstruction framework is based on the three-stage precipitation downscaling approach proposed by Chandler and Wheeler (2002). First, we calibrated our reconstruction using three proxy data sources for 1996-2012: teleconnections, weather station data, and tree ring width time series. Next, the AHCCD and CANGRD precipitation time series between 1951 and 1996 were used to validate the calibrated downscaling model and test the robustness of our reconstructions. Finally, we hindcast our ensemble back to the 1920s when the instrumental rainfall measurements and the well-replicated portion of the MC2 record overlap.

The downscaling framework contains models for precipitation occurrences and amounts. For modelling a daily precipitation event, the occurrences model provides the probability based on the weather conditions or climate proxy information (i.e. tree ring data here) to determine the probability that a precipitation event will occur on that day. Then, the amounts model generates the magnitude of the precipitation event (based on the gamma distribution) conditioned by the weather states and climate proxy information. A summary of the models is given below. Further details and discussion of the approach can be found in Chandler (2006) and Chun (2010).

To determine the occurrence probability ( $p_i$ ) of a precipitation event, a logistic regression model conditioned by weather states and/or climate proxy information is expressed as:

$$\ln\left(\frac{p_i}{1-p_i}\right) = x_i^T \beta$$

where  $p_i$  is the occurrence probability on the  $i^{\text{th}}$  day,  $T$  is a transpose operation and  $\beta$  is a coefficient vector of predictor vector  $x_i$  which can for example be the weather states, previous precipitation days, or proxy climate information.

Using a gamma distribution with a constant dispersion, the expected daily precipitation amount ( $\mu_i$ ) on a wet day can be generated based on weather states, climate proxy, or other predictors:

$$\ln(\mu_i) = \xi_i^T \gamma$$

where  $\xi_i^T$  represents the amounts model predictors and  $\gamma$  is a regression coefficient vector. One of the main advantages of the proposed downscaling approach is its formal inference framework from which we can derive the significance level of the external proxy variables (e.g. tree ring data), when the internal variables such as seasonality and autocorrelation are

considered (Chandler and Wheeler, 2002). In this study, multiple downscaling models with different seasonality and autocorrelation structures were examined. Different external proxy variables included different teleconnection indices and CANGRD maximum and minimum temperature time series, along with tree-ring master curves. The downscaling models were developed using the BERMS precipitation data between 1996 and 2010. Then, using the calibrated downscaling models, an ensemble of 100 time series were simulated from 1920 to 2010, and these results were compared to the CANGRD gridded data, and the AHCCD Prince Albert and Waskesiu Lake station records.

Various downscaling model structures were tested. The downscaling model structures of the Generalised Linear Model (GLM) approach (Chandler and Wheeler, 2002) can be defined in terms of internal structures and external interactions. The former include temporal and site effects. For the three BERMS precipitation time series, Fourier series were used to model the timing (phase) and magnitude of seasonal effects. To account for the temporal autocorrelation within the precipitation time series, previous day precipitation occurrence states and amounts were used as internal variables. Spatial occurrence dependence was introduced by conditioning site probabilities by the weather states (wet or dry) of other sites using logistic regression. The precipitation amount correlations based on distance were modelled by a powered exponential correlation function as in Chandler (2006). A 0.5 mm threshold was used to define precipitation event occurrence. A detailed discussion of different approaches for defining a rainfall event based on thresholds can be found in Yang et al. (2006). The downscaling internal model structure was kept simple so that remaining degrees of freedom could be used for external variables (Table 2).

#### *Episode analysis and extreme value theory*

Tree-ring based reconstructions of annual precipitation (e.g. Biondi, 2014; St. George et al., 2009) are often evaluated using time-series analyses of precipitation duration, magnitude, and

peak. In our proposed approach to reconstruct daily precipitation, the low frequency (decadal) properties of the precipitation observations and simulations were quantified using the analytical framework of Biondi et al. (2008). Within the time series, an “episode” was defined by consecutive anomalies above or below a reference value (cf. Biondi et al., 2002). The episode properties of precipitation time series are related to persistence (i.e. drought characteristics; Biondi et al., 2008). Similar episode analysis approaches have also been widely used in eco-hydroclimatic applications and reconstruction based on dendrochronological data (e.g. Biondi, 2014; Touchan et al., 1999). As this study aimed to reconstruct precipitation time series using tree ring data, we used episode characteristics (duration, magnitude, and peak) defined by Biondi et al. (2008) instead of the traditional hydrological definitions (Chun et al., 2013). Duration is the time length of an episode; magnitude is the sum of all values within an episode, and peak is the absolute maximum value within each episode. Each episode was scored by the ranks of the three characteristics. First, each characteristic was rank-scaled between 0 and 1, where 0 is the score for the lowest rank and 1 for the highest rank, and then the ranks of all three characteristics were summed. The resulting maximum score for one episode was 3. For comparison, the episode analysis was also performed for negative episodes representing dry periods.

Daily rainfall maxima may cause soil saturation, and though rapid saturation leads to runoff, infiltration that recharges soil moisture may have important implications for vegetation (Brooks et al., 2010; Zeppel et al., 2014), and these maxima are studied using extreme value theory (Coles, 2001). Here we used annual daily maximum precipitation to evaluate the quality of the simulated daily reconstruction. The Generalised Extreme Value (GEV) distribution was used to generalise the extreme properties of both observations and simulations (cf. Chun and Wheater, 2012). Based on large number theory, the annual daily maximum distribution converges to the GEV distribution, which is a generalisation of the

Gumbel distribution (Coles, 2001). Therefore, cumulative density functions ( $F(M \leq y_i)$ ) of precipitation maximum ( $y_i$ ) for year  $i$  can be expressed as:

$$F(M \leq y_i) = \exp\left\{-\left[1 + \xi\left(\frac{y_i - \mu}{\sigma}\right)\right]^{-1/\xi}\right\}$$

where  $\mu$ ,  $\sigma$  and  $\xi$  are the location, scale, and shape parameters. When  $\xi$  is equal to zero, the GEV distribution becomes a Gumbel distribution.

## Results

### *Downscaling models*

In developing our downscaling models, we first investigated “plain” models that do not require any external driving variables (such as, e.g. tree rings, climate proxies, or weather states). Although the downscaled annual precipitation ensembles captured the summary precipitation statistics at the BERMS study sites (Figure 3) and enclosed both observations and the CANGRD data (Figure 4; note that the CANGRD data were not used for model fitting), the 99% percentile ranges of the ensemble results were large (i.e. the estimates were uncertain). In this study, our approach is not to reconstruct precipitation beyond the instrumental record, but to converge our simulation results to observed precipitation probability distributions and assess the potential to reconstruct daily precipitation using tree rings (i.e. convergence in the precipitation distribution but not a specific precipitation event). Fig. A1 in Appendix shows that the simulated daily precipitation distributions are similar to the observed daily precipitation distributions. To better constrain the simulated time series tree-ring chronologies, other external variables including ten teleconnection indices (Barnston and Livezey, 1987) and the monthly averaged CANGRD minimum and maximum daily temperature were explored in the precipitation downscaling model analysis.

Based on multiple stepwise comparisons, all teleconnection variables were dropped from the downscaling model. Similarly, CANGRD minimum temperature was insignificant compared to CANGRD maximum temperature, and CANGRD maximum temperature had reduced impact when used in combination with tree ring data. In addition, the model results using CANGRID maximum temperature were erratic with considerable disparity in precipitation values (data not shown). Finally, tree ring data with different time lags were considered, but did not significantly affect the results. Based on these model comparisons, we excluded all proxy data except tree-ring data from the downscaling model.

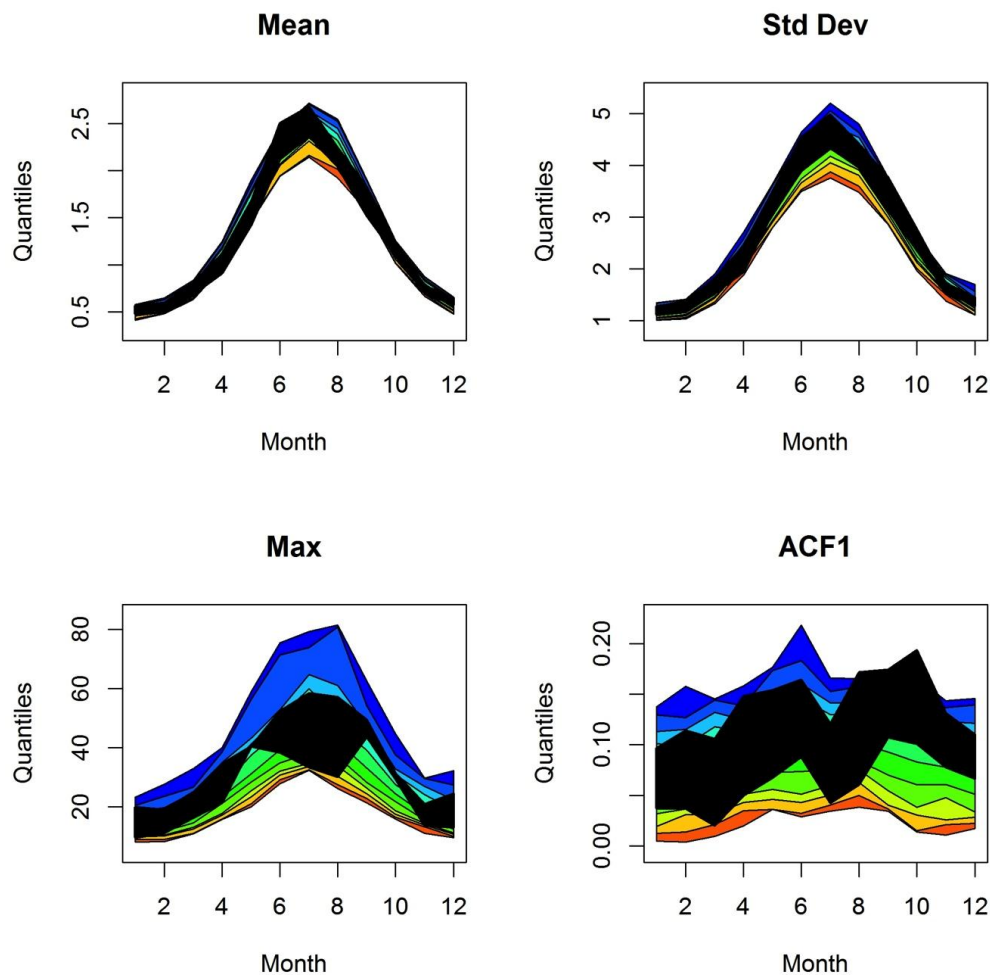


**Figure 3.** Precipitation characteristics from 1996 to 2010. Colour bands show the 1st, 5th, 10th, 25th, 50th, 75th, 90th, 95th and 99th percentiles. The black bands encompassed the observed average precipitation mean, standard deviation, maximum, and autocorrelation. The

maxima varied considerably among years, hence the large spread and curvature in the black bands.

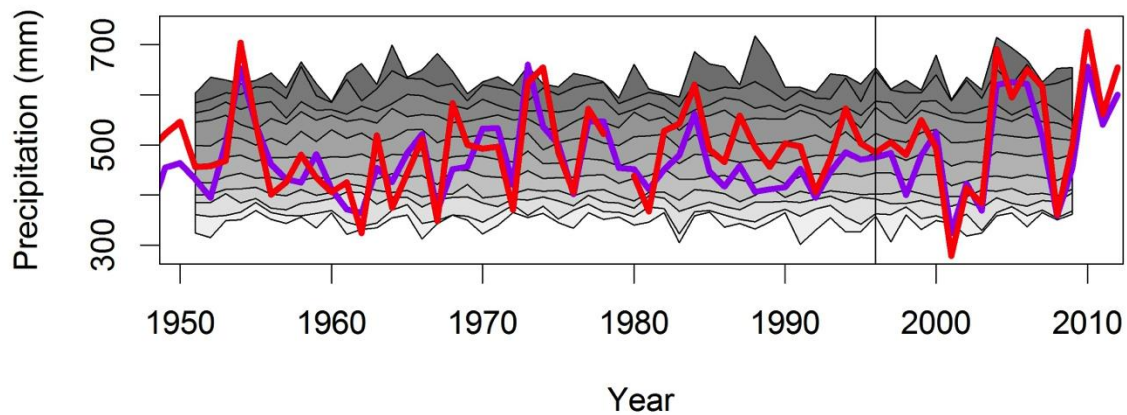


**Figure 4.** The 100-simulation precipitation ensemble plotted against the Prince Albert observations (red line) and the CANGRD data (purple line). The bands show the 1st, 5th, 10th, 25th, 50th, 75th, 90th, 95th and 99th percentiles. The BERMS data after 1996 (vertical black line) were used for calibration, and the simulation before 1996 was used for validation.

**Table 3.** Precipitation model structure without external driving variables. The formulated structure contains two parts: occurrences and amounts models. The seasonal patterns of the models are defined by cosine and sine curves. The autocorrelation structure is defined by the previous day precipitation with a threshold. The simulation results of this model are presented in Figure 4.

#### Occurrences model

1	Constant
2	Daily seasonal effect, cosine component
3	Daily seasonal effect, sine component
4	Previous day precipitation occurrence indicator for daily temporal
5	Precipitation occurrence threshold (0.5 mm)
6	Parameter in the logistic model based on conditional independence

#### Amounts model

1	Constant
2	Daily seasonal effect, cosine component
3	Daily seasonal effect, sine component
4	Previous day precipitation amounts with a logarithm transformation
5	Precipitation occurrence threshold (0.5 mm)
6	Dispersion parameter
7	Three parameters in the correlation function for precipitation

*Influence of tree rings on reconstructed precipitation and the finalised downscaling model*

Compared with annual precipitation time series reconstructed from other proxy data, the ensembles conditioned using tree-rings were more consistent with the observed Prince Albert and CANGRD precipitation time series (Figure 5). The precipitation reconstruction was most poorly constrained during extended periods of high forest pest severity (e.g., 1962–1965, 1978–1982, and 2001–2004). Nonetheless, the simulations captured extremes in the duration, maximum, and episode scores, typically enclosing the observed values for the strongest 10 episodes (Figure 6). The simulation also performed well for absolute episode magnitude, except for the strongest episodes during which the simulation was higher than the observations. A similar analysis was completed for the negative episodes (i.e. the dry events), with comparable results (Appendix). Based on the above results, our final model for precipitation reconstruction only includes tree-ring data and the plain downscaling model in Table 3.

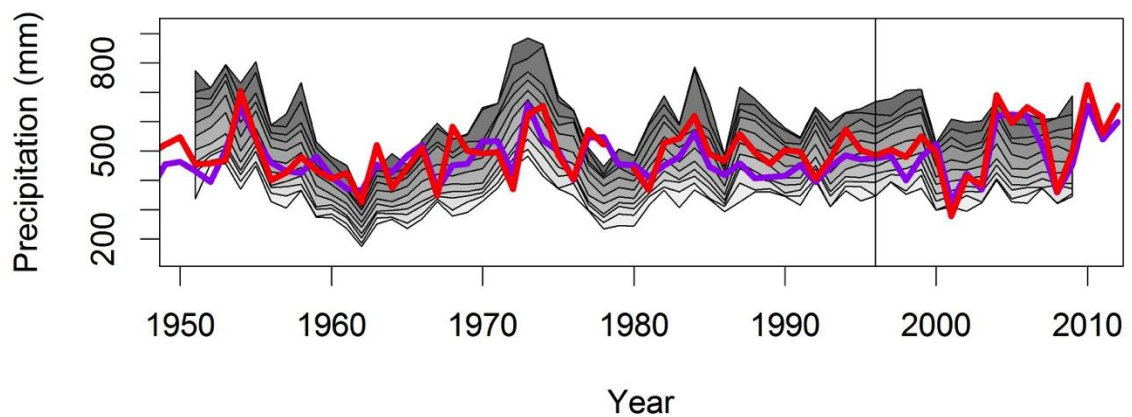


**Figure 5.** The annual precipitation simulation ensemble conditioned by tree-ring data. The 100-simulation ensemble was plotted against the Prince Albert observations (red line) and the CANGRD data (purple line). The bands show the 1st, 5th, 10th, 25th, 50th, 75th, 90th, 95th and 99th percentiles. The BERMS data after 1996 (vertical black line) were used for calibration, and the simulation between 1951 and 1996 was used for validation.

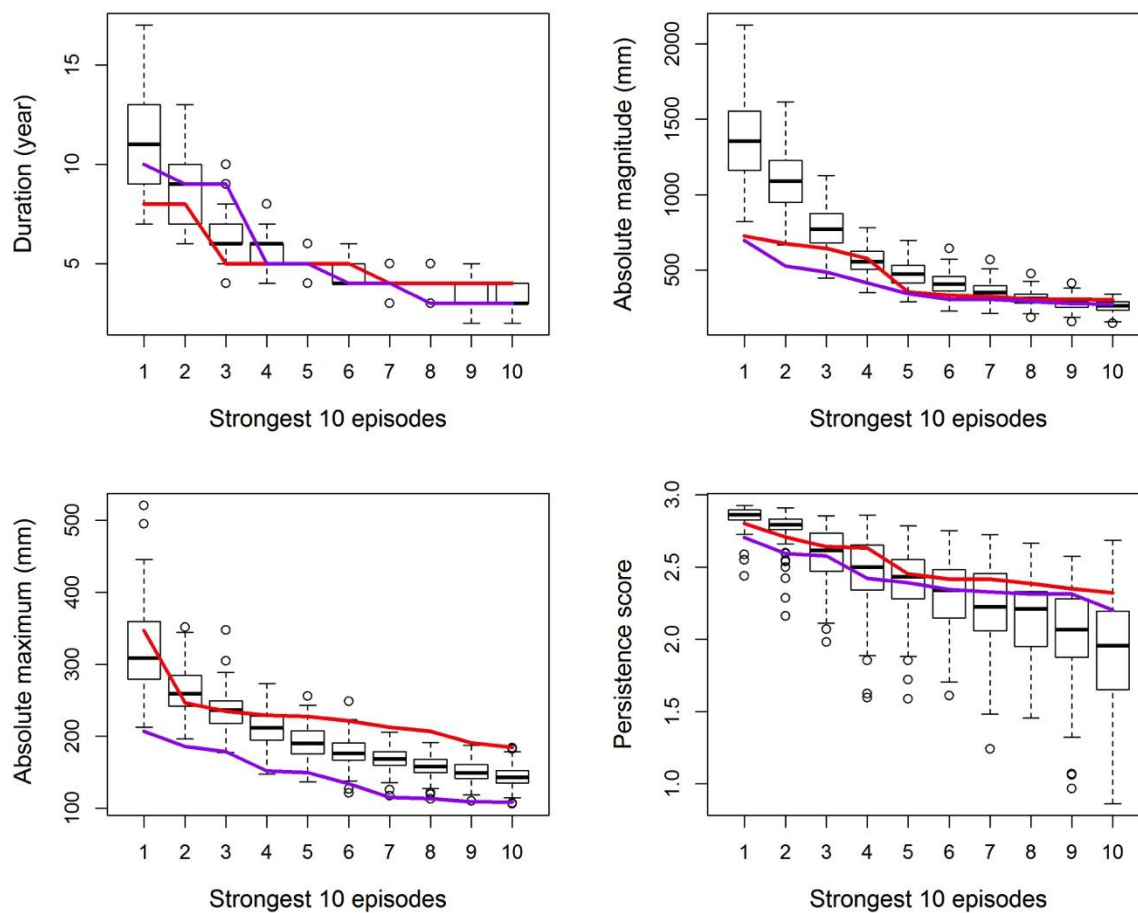


**Figure 6.** Summary of the persistent precipitation properties and downscaled results based on episode characteristics as defined by Biondi et al. (2008). The boxplots represent the simulation results plotted against the Prince Albert observations (red line) and CANGRD data (purple line).

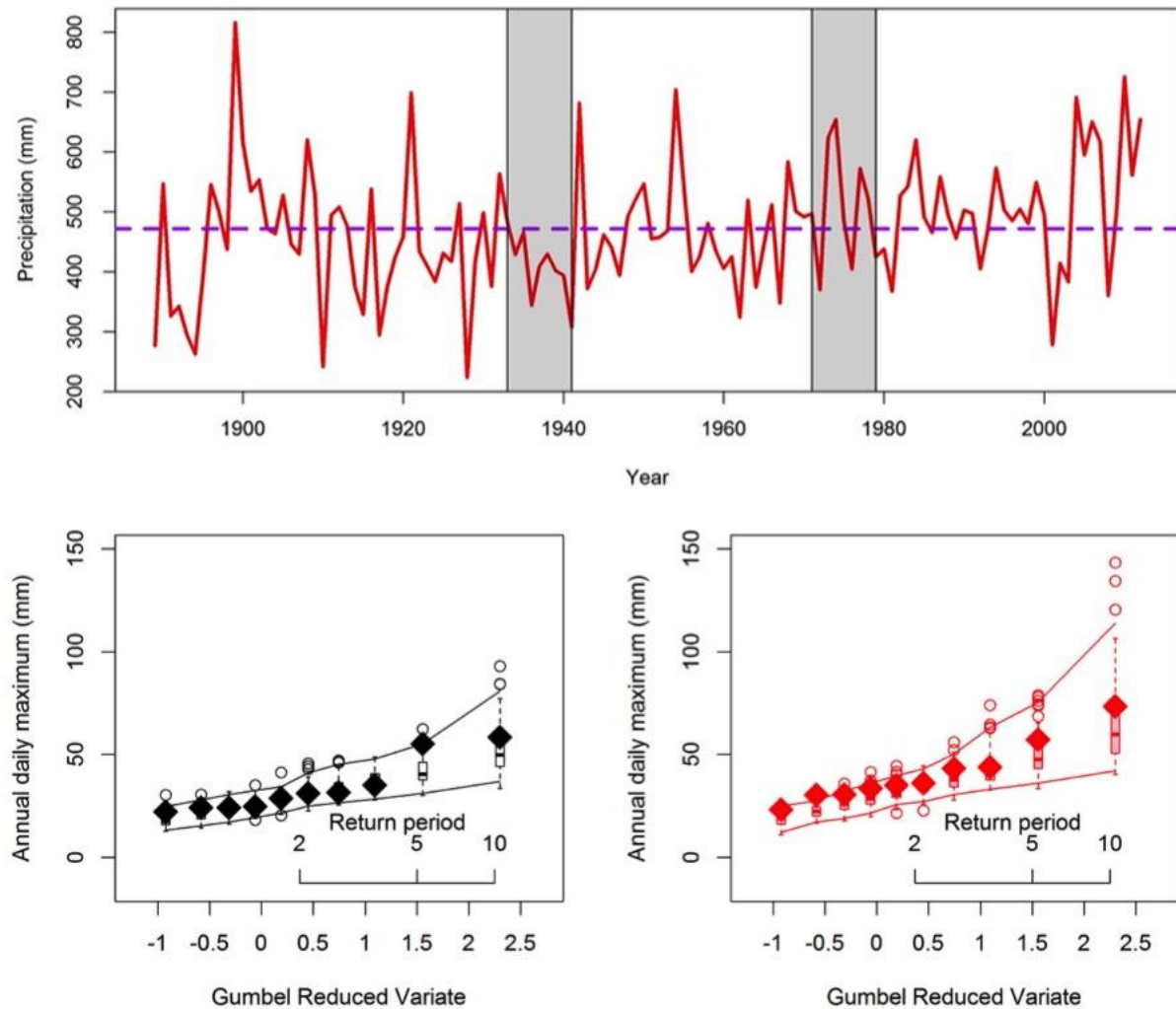


**Figure 7.** Wet (1971-1979) and dry (1933-1941) periods (grey shading) were identified (upper panel) and analysed for daily extremes. Gumbel plots of the daily annual extremes of the dry (black, lower left) and wet periods (red, lower right). Gumbel plots are a graphical method widely used by hydrologists to quantify extreme characteristics. The dots are the observed annual daily maxima for the wet and dry periods. The boxplots are corresponding annual daily maxima of the simulation results. For easy interpretation, the 95% percentiles of the simulation results (solid lines) are also included. Generally, the simulations are considered to be reasonable if the observations (dots) are within the 95% percentiles envelope.

#### *Precipitation extremes analysis*

For annual daily extreme analysis (see §Episode analysis and extreme value theory) we identified wet (1971-1979) and dry (1933-1941) periods in the CANGRD annual precipitation data (Figure 7a). The estimated GEV location parameter of the Prince Albert maxima for the wet period was 33 mm, which was significantly higher than the location parameter for the dry period (26 mm) with 95% confidence intervals from 22 mm to 30 mm.

Our results suggest significant differences between wet and dry periods, as indicated by the Prince Albert GEV distributions. While the precipitation series in the dry and wet periods were different, the simulated downscaled precipitation ensemble was consistent with the observed Prince Albert extremes. The 95% confidence bounds derived from the simulated ensemble results enclosed both high and low Prince Albert precipitation amounts (Figure 7.) The Prince Albert GEV location parameter for the wet period (33mm) was also not significantly different from the simulated ensemble wet period parameter (29mm), with 95% parameter confidence intervals between 20 and 43mm. Furthermore, we obtained similar results when the simulation envelopes were presented together (Figure 8). Overall, as would be expected, the simulated extreme envelope of the wet period was higher than that of the dry period.

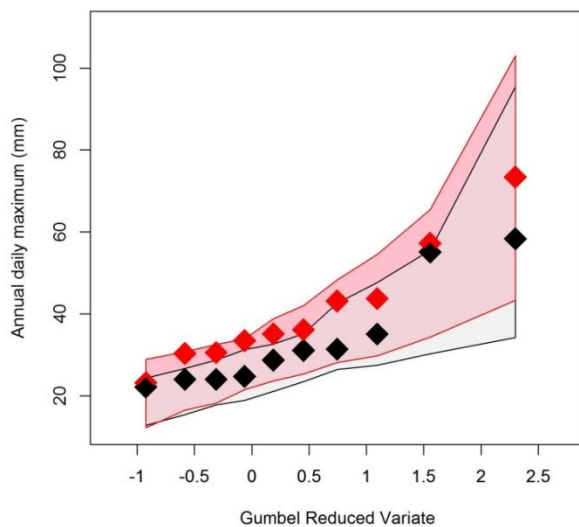


**Figure 8.** Gumbel plots of the daily annual extremes of wet (1971-1979; red) and dry (1933-1941; black) periods combined. The dots show the annual daily maxima and the shading areas show the 95% percentiles. Overall, the wet period simulation shading is slightly higher than the dry period simulation shading.

## Discussion

Most existing theoretical models for episode (defined by consecutive anomalies above or below a reference value) characteristics have paid only limited attention to the time series covariance structure (see Biondi et al., 2002). Therefore, instead of using stationary episode distributions, we derived episode characteristics (magnitude, peak, and duration) and compared these metrics between the observed precipitation time series and simulated GLM ensembles. Our study builds upon previous annual hydroclimatic modelling studies (e.g. Griffin et al., 2013; Kames et al., 2016; Yang et al., 2014) by evaluating daily maxima in precipitation. The episodes derived from the simulated precipitation ensembles allowed us to model the autocorrelation structure within the precipitation reconstruction. Moreover, the intervals (i.e. uncertainty) of a particular rank or exceedance probability of an event can also be computed from the ensemble. Cross-temporal-scale precipitation reconstructions based on the current approach should be further explored.

Although we successfully used tree ring data to reconstruct the precipitation time series in the western boreal forest of central Saskatchewan, the results could be improved through the inclusion of ecological factors affecting ring width. Severe insect outbreaks in the early 1960s and late 1970s reduced ensemble levels to below the observational record (Figures 2, 5). Jack pine budworm (*Choristoneura pinus pinus* Free.) and aspen defoliator outbreaks (e.g., *Malacosoma* spp.) during the early 1960s and late 1970s notably reduced growth rates of both jack pine and trembling aspen across much of central Canada (Hogg et al., 2005; National Forestry Database, 2015; Volney, 1998). Though evidence of spruce budworm outbreaks exist for central Canada (Lacey and Dech, 2012), these outbreaks are typically limited to stands with some balsam fir (Gray, 2013) and fir was absent at our study sites. Precipitation simulations reflect at least two major pest outbreaks between 1920 and 2010. During these outbreaks, tree radial growth increments were distinctly low, causing the

ensemble precipitation reconstructions to be lower than the corresponding Prince Albert and Waskesiu observations. Currently, the reconstruction model did not explicitly include outbreaks as an external driver. It is imperative that we understand and include the influence of ecological disturbances on tree growth in order to accurately hindcast precipitation time series beyond the instrumental record. The downscaling model can be improved by incorporating reliable and long ecological outbreak chronologies.

The current analysis focused on temporal downscaling. Tree-ring data can also be used to understand spatial climate relationships (e.g. Meko et al., 1993) and provide regional context to precipitation variability (Dettinger et al., 1998). Recent modelling breakthroughs have used tree ring data to both generate gridded products (Cook and Krusic, 2004) as well as finer-scale information within grids (Biondi, 2014). Gridded precipitation products can be produced by downscaling temporal and spatial tree ring data simultaneously (Biondi, 2014). Instead of using a regional master tree ring chronology, individual tree species and sub-regional tree ring data may be used for spatial analysis. By further developing downscaling approaches using various paleoenvironmental time series, we may develop products that can be used to evaluate historical simulations from global climate models in the context of a changing climate. A study similar to Themeßl et al. (2011) could be further developed along the method investigated in this study for other biomes such as tropical and subtropical forests.

The downscaling approach investigated here could also be applied to centennial and longer tree-ring time series available in the Canadian boreal forest (e.g. Sauchyn et al., 2015). Instead of using instrumental data products such as CANGRD temperature, other paleoenvironmental time series such as carbon isotopes (Youfeng et al., 2008) can be used as the driving downscaling proxies. One of the advantages of our proposed framework is its formal inference, which allows us to statistically test the significance of environmental variables. Combining instrumental and proxy records together with projected climate model

simulations has proven useful for advising water resource managers (Biondi, 2014), though additional studies are necessary due to stochastic events (e.g. insect outbreaks) potentially obscuring the hydroclimatic signal in regional tree ring chronologies. Biotic influences related to disturbance and competition are important determinants of tree growth, and recent evidence suggests that internal community-level processes may be as important as external climatic factors in driving tree growth dynamics (Bond-Lamberty et al., 2014; Zhang et al., 2015). Moreover, pests or pathogens may cause tree growth patterns that are distinct from direct climate effects (Hogg et al., 2002; Mamet et al., 2015; McDowell et al., 2011). Previous studies have proven the value of annual reconstructions of hydroclimatic variability for diagnosing ongoing and future climatic change (Au and Tardif, 2012; Beriault and Sauchyn, 2006; Biondi, 2014; Cook et al., 2015). Our downscaling approach provides a means of studying finer scale characteristics of hydroclimatic variability by incorporating tree ring width data to simulate underlying stochastic processes in daily precipitation reconstructions. Future work should include evaluation of this method using tree ring width series and quantitative assessment of abiotic influences (e.g. insect outbreaks) to reduce any non-climatic signal present in precipitation reconstructions.

## **Conclusions**

Tree ring time series are a rich source of hydroclimate information for historic precipitation time series reconstruction. Here we have provided a framework that uses 15 years of high-quality precipitation data from a regional flux tower network to simulate half-century precipitation ensembles. By incorporating tree ring width information, we significantly improved our daily-scale reconstructions of rainfall extremes. Our framework provides a means for studying historical hydrological conditions such as droughts and flooding in the south Canadian boreal forest, with the caveat that pest outbreaks may at times obscure the

drought signal. By integrating the results here to existing and future natural resource management schemes, our framework may provide a valuable platform from which to place ongoing and future fine-scale changes in precipitation into a broader historical context.

### **Acknowledgements**

This research was supported by a Global Institute for Water Security fellowship and a Hong Kong Baptist University Faculty Research Grant (FRG2/15-16/085) to KPC, an NSERC Discovery Grant to JFJ, the Climate Change and Atmospheric Research program, the Canada Excellence Research Chair (HW) in Water Security at the University of Saskatchewan, and through a Garfield-Weston Postdoctoral Fellowship scholarship to SDM. The efforts of B Charry, E J Tissier, A Truchon-Savard, and M Voicu were crucial for fieldwork completion and sample preparation.

## References

- Au, R., Tardif, J.C., 2012. Drought signals inferred from ring-width and stable carbon isotope chronologies from *Thuja occidentalis* trees growing at their northwestern distribution limit, central Canada. *Canadian Journal of Forest Research* 42, 517-531.
- Barnston, A.G., Livezey, R.E., 1987. Classification, seasonality and persistence of low-frequency atmospheric circulation patterns. *Monthly Weather Review* 115, 1083-1126.
- Barr, A.G., van der Kamp, G., Black, T.A., McCaughey, J.H., Nesic, Z., 2012. Energy balance closure at the BERMS flux towers in relation to the water balance of the White Gull Creek watershed 1999–2009. *Agricultural and Forest Meteorology* 153, 3-13.
- Berriault, A.L., Sauchyn, D.J., 2006. Tree-ring reconstructions of streamflow in the Churchill River Basin, northern Saskatchewan. *Canadian Water Resources Journal* 31, 249-262.
- Biondi, F., 2014. Dendroclimatic reconstruction at kilometer-scale grid points: A case study from the Great Basin of North America. *Journal of Hydrometeorology* 15, 891-906.
- Biondi, F., Kozubowski, T.J., Panorska, A.K., 2002. Stochastic modeling of regime shifts. *Climate Research* 23, 23-30.
- Biondi, F., Kozubowski, T.J., Panorska, A.K., Saito, L., 2008. A new stochastic model of episode peak and duration for eco-hydro-climatic applications. *Ecological Modelling* 211, 383-395.
- Bond-Lamberty, B., Rocha, A.V., Calvin, K., Holmes, B., Wang, C., Goulden, M.L., 2014. Disturbance legacies and climate jointly drive tree growth and mortality in an intensively studied boreal forest. *Global Change Biology*, 216–227.
- Bradley, R.S., 2015. *Paleoclimatology: Reconstructing Climates of the Quaternary* Third ed. Academic Press, Oxford, UK.
- Briffa, K.R., Jones, P.D., 1990. Basic chronology statistics and assessment, in: Cook, E.R., Kairiukstis, L.A. (Eds.), *Methods of dendrochronology: applications in the environmental sciences*. Kluwer Academic Publishers, Dordrecht, The Netherlands, pp. 137-152.
- Brooks, J.R., Barnard, H.R., Coulombe, R., McDonnell, J.J., 2010. Ecohydrologic separation of water between trees and streams in a Mediterranean climate. *Nature Geoscience* 3, 100–104.
- Bunn, A., Korpela, M., Biondi, F., Campelo, F., Mérian, P., Mudelsee, M., Qeadan, F., Schulz, M., Zang, C., 2014. dplR: Dendrochronology Program Library in R. R package version 1.6.0., <http://CRAN.R-project.org/package=dplR>.
- Burns, R.M., Honkala, B.H., 1990. *Silvics of North America*. 1. Conifers. U.S. Department of Agriculture, Forest Service, Washington, D.C.
- Chandler, R.E., 2006. *GLIMCLIM: Generalized linear modelling for daily climate time series (software and user guide)*. University College London, London, UK.
- Chandler, R.E., Wheeler, H.S., 2002. Analysis of rainfall variability using generalized linear models: A case study from the west of Ireland. *Water Resources Research* 38, 10-11–10-11.

- Chen, L., Huang, J.-G., Stadt, K.J., Comeau, P.G., Zhai, L., Dawson, A., Alam, S.A., 2017. Drought explains variation in the radial growth of white spruce in western Canada. *Agricultural and Forest Meteorology* 233, 133-142.
- Chhin, S., Wang, G., 2016. Climatic sensitivity of a mixed forest association of white spruce and trembling aspen at their southern range limit. *Forests* 7, 235.
- Chun, K.P., 2010. Statistical downscaling of climate model outputs for hydrological extremes. Imperial College, London, U.K.
- Chun, K.P., Wheeler, H., 2012. An extreme analysis for the 2010 precipitation event at the South of Saskatchewan Prairie. *Global NEST Journal* 14, 311–324.
- Chun, K.P., Wheeler, H., Onof, C., 2013. Prediction of the impact of climate change on drought: an evaluation of six UK catchments using two stochastic approaches. *Hydrological Processes* 27, 1600-1614.
- Coles, S., 2001. Extremes of dependent sequences, An introduction to statistical modeling of extreme values. Springer, London, U.K., pp. 92-104.
- Cook, E.R., Krusic, P.J., 2004. The North American Drought Atlas. Lamont-Doherty Earth Observatory and the National Science Foundation.
- Cook, E.R., Seager, R., Kushnir, Y., Briffa, K.R., Büntgen, U., Frank, D., Krusic, P.J., Tegel, W., van der Schrier, G., Andreu-Hayles, L., Baillie, M., Baittinger, C., Bleicher, N., Bonde, N., Brown, D., Carrer, M., Cooper, R., Čufar, K., Dittmar, C., Esper, J., Griggs, C., Gunnarson, B., Günther, B., Gutierrez, E., Haneca, K., Helama, S., Herzig, F., Heussner, K.-U., Hofmann, J., Janda, P., Kontic, R., Köse, N., Kyncl, T., Levanič, T., Linderholm, H., Manning, S., Melvin, T.M., Miles, D., Neuwirth, B., Nicolussi, K., Nola, P., Panayotov, M., Popa, I., Rothe, A., Seftigen, K., Seim, A., Svarva, H., Svoboda, M., Thun, T., Timonen, M., Touchan, R., Trotsiuk, V., Trouet, V., Walder, F., Ważny, T., Wilson, R., Zang, C., 2015. Old World megadroughts and pluvials during the Common Era. *Science Advances* 1, E1500561.
- Dettinger, M.D., Cayan, D.R., Diaz, H.F., Meko, D.M., 1998. North–south precipitation patterns in western North America on interannual-to-decadal timescales. *Journal of Climate* 11, 3095-3111.
- Drobyshev, I., Simard, M., Bergeron, Y., Hofgaard, A., 2010. Does soil organic layer thickness affect climate–growth relationships in the black spruce boreal ecosystem? *Ecosystems* 13, 556-574.
- Elshorbagy, A., Wagener, T., Razavi, S., Sauchyn, D., 2016. Correlation and causation in tree-ring-based reconstruction of paleohydrology in cold semiarid regions. *Water Resources Research* 52, 7053-7069.
- Fritts, H.C., 2001. Tree rings and climate. The Blackburn Press, Caldwell, New Jersey.
- Girardin, M.-P., Tardif, J., 2005. Sensitivity of tree growth to the atmospheric vertical profile in the Boreal Plains of Manitoba, Canada. *Canadian Journal of Forest Research* 35, 48-64.

- Girardin, M.P., Hogg, E.H., Bernier, P.Y., Kurz, W.A., Guo, X.J., Cyr, G., 2016. Negative impacts of high temperatures on growth of black spruce forests intensify with the anticipated climate warming. *Global Change Biology* 22, 627-643.
- Gray, D.R., 2013. The influence of forest composition and climate on outbreak characteristics of the spruce budworm in eastern Canada. *Canadian Journal of Forest Research* 43, 1181-1195.
- Gray, S.T., Betancourt, J.L., Fastie, C.L., Jackson, S.T., 2003. Patterns and sources of multidecadal oscillations in drought-sensitive tree-ring records from the central and southern Rocky Mountains. *Geophysical Research Letters* 30, 1316.
- Griffin, D., Woodhouse, C.A., Meko, D.M., Stahle, D.W., Faulstich, H.L., Carrillo, C., Touchan, R., Castro, C.L., Leavitt, S.W., 2013. North American monsoon precipitation reconstructed from tree-ring latewood. *Geophysical Research Letters* 40, 954-958.
- Griffis, T.J., Black, T.A., Morgenstern, K., Barr, A.G., Nestic, Z., Drewitt, G.B., Gaumont-Guay, D., McCaughey, J.H., 2003. Ecophysiological controls on the carbon balances of three southern boreal forests. *Agricultural and Forest Meteorology* 117, 53-71.
- Hall, F.G., Knapp, D.E., Huemmrich, K.F., 1997. Physically based classification and satellite mapping of biophysical characteristics in the southern boreal forest. *Journal of Geophysical Research: Atmospheres* 102, 29567-29580.
- Hansen, M.C., Potapov, P.V., Moore, R., Hancher, M., Turubanova, S.A., Tyukavina, A., Thau, D., Stehman, S.V., Goetz, S.J., Loveland, T.R., Kommareddy, A., Egorov, A., Chini, L., Justice, C.O., Townshend, J.R.G., 2013. High-resolution global maps of 21st-century forest cover change. *Science* 342, 850-853.
- Hofgaard, A., Tardif, J., Bergeron, Y., 1999. Dendroclimatic response of *Picea mariana* and *Pinus banksiana* along a latitudinal gradient in the eastern Canadian boreal forest. *Canadian Journal of Forest Research* 29, 1333-1346.
- Hogg, E.H., Brandt, J.P., Kochtubajda, B., 2002. Growth and dieback of aspen forests in northwestern Alberta, Canada, in relation to climate and insects. *Canadian Journal of Forest Research* 32, 823-832.
- Hogg, E.H., Brandt, J.P., Kochtubajda, B., 2005. Factors affecting interannual variation in growth of western Canadian aspen forests during 1951–2000. *Canadian Journal of Forest Research* 35, 611–622.
- Holmes, R.L., 1992. Dendrochronology program library, version 1992-1. University of Arizona.
- Huang, J., Tardif, J.C., Bergeron, Y., Denneler, B., Berninger, F., Girardin, M.P., 2010. Radial growth response of four dominant boreal tree species to climate along a latitudinal gradient in the eastern Canadian boreal forest. *Global Change Biology* 16, 711-731.
- Huang, J.-G., Bergeron, Y., Berninger, F., Zhai, L., Tardif, J.C., Denneler, B., 2013. Impact of future climate on radial growth of four major boreal tree species in the eastern Canadian boreal forest. *PLoS ONE* 8, e56758.

- Ireson, A.M., Barr, A.G., Johnstone, J.F., Mamet, S.D., van der Kamp, G., Whitfield, C.J., Michel, N.L., North, R.L., Westbrook, C.J., DeBeer, C., Chun, K.P., Nazemi, A., Sagin, J., 2015. The changing water cycle: the Boreal Plains ecozone of Western Canada. *Wiley Interdisciplinary Reviews: Water* 2, 505–521.
- Kames, S., Tardif, J.C., Bergeron, Y., 2016. Continuous earlywood vessels chronologies in floodplain ring-porous species can improve dendrohydrological reconstructions of spring high flows and flood levels. *Journal of Hydrology* 534, 377-389.
- Köcher, P., Horna, V., Leuschner, C., 2012. Environmental control of daily stem growth patterns in five temperate broad-leaved tree species. *Tree Physiology* 32, 1021-1032.
- Lacey, M.E., Dech, J.P., 2012. Comparison of black spruce (*Picea mariana*) radial growth reduction in different soil moisture regimes during a spruce budworm (*Choristoneura fumiferana*) outbreak. *Canadian Journal of Forest Research* 42, 1410-1419.
- Lapointe-Garant, M.-P., Huang, J.-G., Gea-Izquierdo, G., Raulier, F., Bernier, P., Berninger, F., 2010. Use of tree rings to study the effect of climate change on trembling aspen in Québec. *Global Change Biology* 16, 2039-2051.
- Leonelli, G., Denneler, B., Bergeron, Y., 2008. Climate sensitivity of trembling aspen radial growth along a productivity gradient in northeastern British Columbia, Canada. *Canadian Journal of Forest Research* 38, 1211-1222.
- Mallett, K.I., Volney, W.J.A., 1990. Relationships among jack pine budworm damage, selected tree characteristics, and *Armillaria* root rot in jack pine. *Canadian Journal of Forest Research* 20, 1791-1795.
- Mamet, S.D., Chun, K.P., Metsaranta, J.M., Barr, A.G., Johnstone, J.F., 2015. Tree rings provide early warning signals of jack pine mortality across a moisture gradient in the southern boreal forest. *Environmental Research Letters* 10, 084021.
- Maraun, D., Wetterhall, F., Ireson, A.M., Chandler, R.E., Kendon, E.J., Widmann, M., Brienen, S., Rust, H.W., Sauter, T., Themeßl, M., Venema, V.K.C., Chun, K.P., Goodess, C.M., Jones, R.G., Onof, C., Vrac, M., Thiele-Eich, I., 2010. Precipitation downscaling under climate change: Recent developments to bridge the gap between dynamical models and the end user. *Reviews of Geophysics* 48, RG3003.
- McDowell, N.G., Beerling, D.J., Breshears, D.D., Fisher, R.A., Raffa, K.F., Stitt, M., 2011. The interdependence of mechanisms underlying climate-driven vegetation mortality. *Trends in Ecology & Evolution* 26, 523-532.
- Meko, D., Cook, E.R., Stahle, D.W., Stockton, C.W., Hughes, M.K., 1993. Spatial patterns of tree-growth anomalies in the United States and southeastern Canada. *Journal of Climate* 6, 1773-1786.
- Meko, D.M., Stockton, C.W., Blasing, T.J., 1985. Periodicity in tree rings from the corn belt. *Science* 229, 381–384.
- Milewska, E., Hopkinson, R.F., Nütsoo, A., 2005. Evaluation of geo-referenced grids of 1961–1990 Canadian temperature and precipitation normals. *Atmosphere-Ocean* 43, 49–75.

- National Forestry Database, 2015. Forest Insects—National Tables, Table 4.1, Area within which moderate to severe defoliation occurs including area of beetle-killed trees by insects and province/territory, 1975–2013. Natural Resources Canada, Canadian Forest Service.
- Peng, C., Ma, Z., Lei, X., Zhu, Q., Chen, H., Wang, W., Liu, S., Li, W., Fang, X., Zhou, X., 2011. A drought-induced pervasive increase in tree mortality across Canada's boreal forests. *Nature Climate Change* 1, 467-471.
- Pepin, S., Plamondon, A., Britel, A., 2002. Water relations of black spruce trees on a peatland during wet and dry years. *Wetlands* 22, 225-233.
- Pisaric, M.F.J., St-Onge, S.M., Kokelj, S.V., 2009. Tree-ring reconstruction of early-growing season precipitation from Yellowknife, Northwest Territories, Canada. *Arctic, Antarctic, and Alpine Research* 41, 486-496.
- Razavi, S., Elshorbagy, A., Wheeler, H., Sauchyn, D., 2015. Toward understanding nonstationarity in climate and hydrology through tree ring proxy records. *Water Resources Research* 51, 1813-1830.
- Razavi, S., Elshorbagy, A., Wheeler, H., Sauchyn, D., 2016. Time scale effect and uncertainty in reconstruction of paleo-hydrology. *Hydrological Processes* 30, 1985-1999.
- Rehfeldt, G.E., Ferguson, D.E., Crookston, N.L., 2009. Aspen, climate, and sudden decline in western USA. *Forest Ecology and Management* 258, 2353-2364.
- Sauchyn, D.J., St-Jacques, J.-M., Luckman, B.H., 2015. Long-term reliability of the Athabasca River (Alberta, Canada) as the water source for oil sands mining. *Proceedings of the National Academy of Sciences* 112, 12621-12626.
- Sonia, S., Morin, H., Krause, C., 2011. Long-term spruce budworm outbreak dynamics reconstructed from subfossil trees. *Journal of Quaternary Science* 26, 734-738.
- St. George, S., Meko, D.M., Girardin, M.-P., MacDonald, G.M., Nielsen, E., Pederson, G.T., Sauchyn, D.J., Tardif, J.C., Watson, E., 2009. The tree-ring record of drought on the Canadian prairies. *Journal of Climate* 22, 689-710.
- Thiemeßl, M.J., Gobiet, A., Leuprecht, A., 2011. Empirical-statistical downscaling and error correction of daily precipitation from regional climate models. *International Journal of Climatology* 31, 1530-1544.
- Touchan, R., Meko, D., Hughes, M.K., 1999. A 396-year reconstruction of precipitation in southern Jordan. *Journal of the American Water Resources Association* 35, 49-59.
- Viereck, L.A., Johnston, W.F., 1990. *Picea mariana* (Mill.) B.S.P, *Silvics of North America*. 1. Conifers. U.S. Department of Agriculture, Forest Service.
- Vincent, L.A., Wang, X.L., Milewska, E.J., Wan, H., Yang, F., Swail, V., 2012. A second generation of homogenized Canadian monthly surface air temperature for climate trend analysis. *Journal of Geophysical Research: Atmospheres* 117, D18110.
- Volney, W.J.A., 1988. Analysis of historic jack pine budworm outbreaks in the Prairie provinces of Canada. *Canadian Journal of Forest Research* 18, 1152-1158.

Volney, W.J.A., 1998. Ten-year tree mortality following a jack pine budworm outbreak in Saskatchewan. *Canadian Journal of Forest Research* 28, 1784-1793.

Walker, X., Johnstone, J.F., 2014. Widespread negative correlations between black spruce growth and temperature across topographic moisture gradients in the boreal forest. *Environmental Research Letters* 9, 064016.

Westwood, A.R., Conciatori, F., Tardif, J.C., Knowles, K., 2012. Effects of *Armillaria* root disease on the growth of *Picea mariana* trees in the boreal plains of central Canada. *Forest Ecology and Management* 266, 1-10.

Yang, B., Qin, C., Wang, J., He, M., Melvin, T.M., Osborn, T.J., Briffa, K.R., 2014. A 3,500-year tree-ring record of annual precipitation on the northeastern Tibetan Plateau. *Proceedings of the National Academy of Sciences* 111, 2903-2908.

Yang, C., Chandler, R.E., Isham, V.S., Wheeler, H.S., 2006. Quality control for daily observational rainfall series in the UK. *Water and Environment Journal* 20, 185-193.

Youfeng, N., Weiguo, L., Zhisheng, A., 2008. A 130-ka reconstruction of precipitation on the Chinese Loess Plateau from organic carbon isotopes. *Palaeogeography, Palaeoclimatology, Palaeoecology* 270, 59-63.

Zeppel, M.J.B., Wilks, J.V., Lewis, J.D., 2014. Impacts of extreme precipitation and seasonal changes in precipitation on plants. *Biogeosciences* 11, 3083-3093.

Zhang, J., Huang, S., He, F., 2015. Half-century evidence from western Canada shows forest dynamics are primarily driven by competition followed by climate. *Proceedings of the National Academy of Sciences* 112, 4009-4014.

## Appendix A.

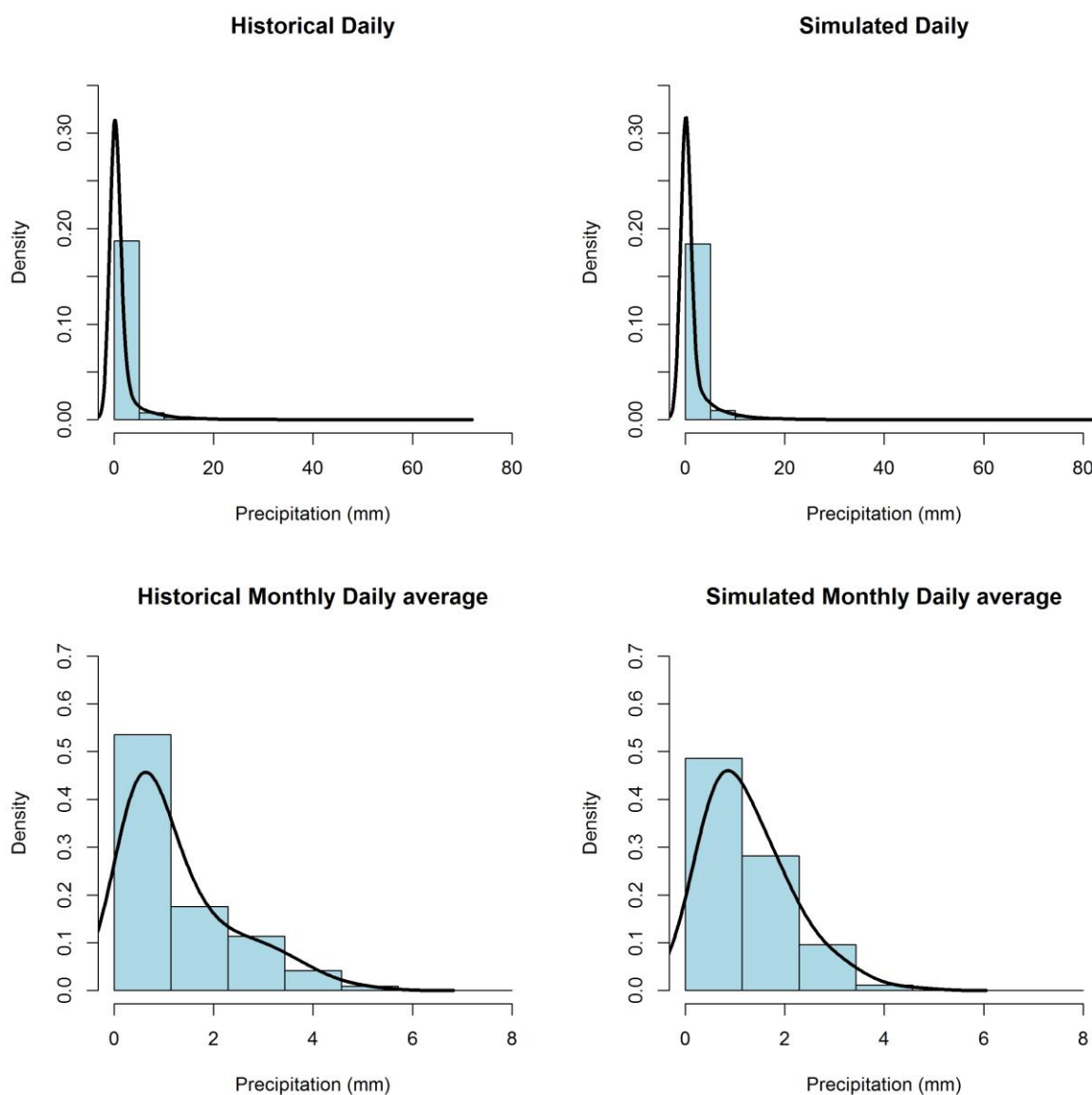


**Fig. A1.** The histograms (bars) and the corresponding density curves (black lines) of daily and monthly average precipitation data for both historical observations and model simulations to show the convergence of the observed and modelled precipitation distributions.

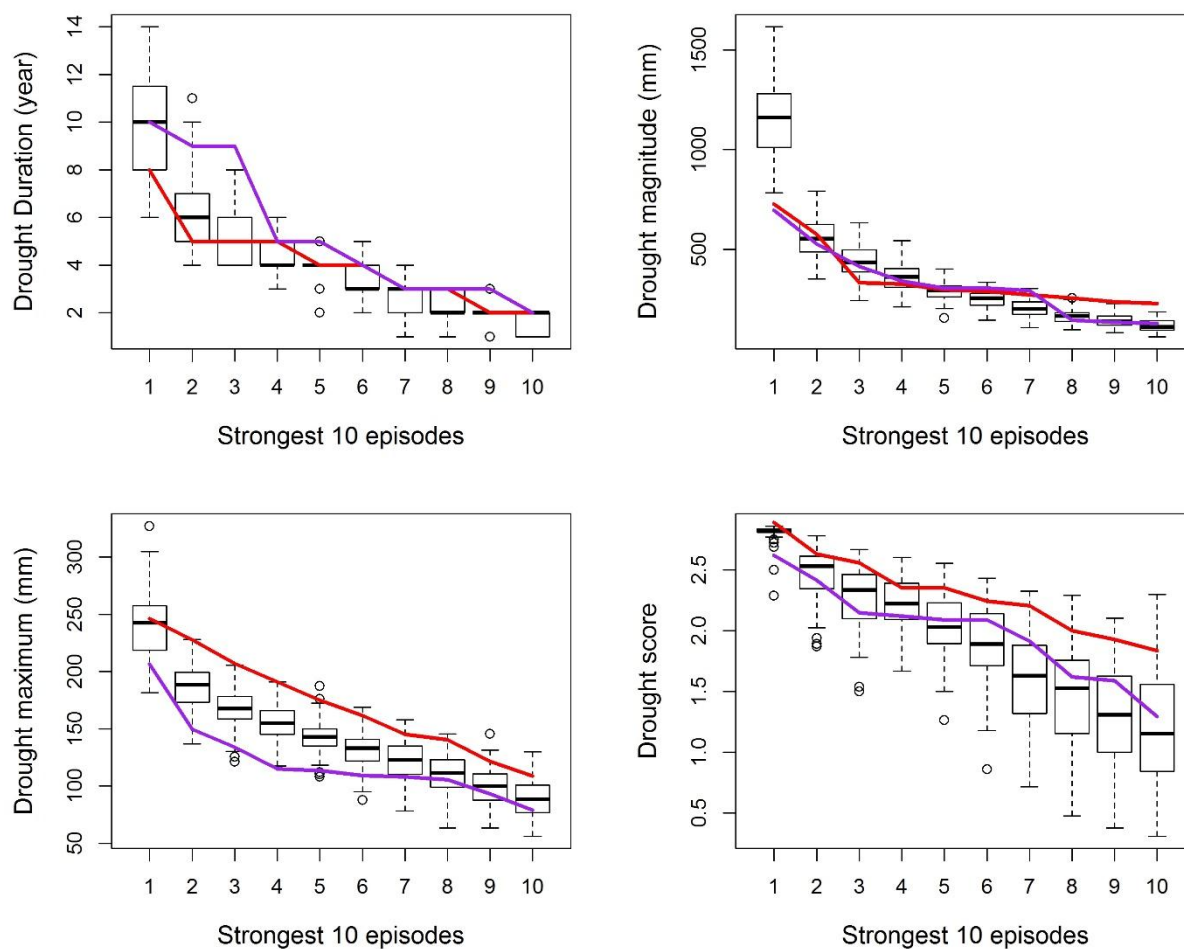


**Fig. A2.** Summary of the persistent observation properties and downscaled results based on only the negative consecutive anomalies below a reference value (i.e. the dry events) (cf. Biondi et al., 2002; Dracup et al., 1980). The boxplots are the simulation results plotted against the Prince Albert observations (red line) and CANGRD data (purple line).

**References**

Biondi, F., Kozubowski, T.J., Panorska, A.K., 2002. Stochastic modeling of regime shifts. *Climate Research* 23, 23-30.

Dracup, J.A., Lee, K.S., Paulson, E.G., 1980. On the definition of droughts. *Water Resources Research* 16, 297-302.